

# Solid-state NMR investigation of sodium nucleotide complexes<sup>†</sup>

Christopher V. Grant,<sup>1</sup> Dan McElheny,<sup>2</sup> Veronica Frydman<sup>3</sup> and Lucio Frydman<sup>3\*</sup>

<sup>1</sup> Department of Chemistry and Biochemistry, University of California, San Diego, La Jolla, CA 92093, USA

<sup>2</sup> Department of Biochemistry and Molecular Biology, The University of Chicago, Chicago, IL 60637, USA

<sup>3</sup> Weizmann Institute of Science, Rehovot, 76100, Israel

Received 31 August 2005; Revised 7 October 2005; Accepted 14 October 2005

Solid-state NMR has been used to analyze the chemical environments of sodium sites in powdered crystalline samples of sodium nucleotide complexes. Three of the studied complexes have been previously characterized structurally by crystallography (disodium deoxycytidine-5'-monophosphate heptahydrate, disodium deoxyuridine-5'-monophosphate pentahydrate and disodium adenosine-5'-triphosphate trihydrate). For these salts, the nuclear quadrupole coupling parameters measured by <sup>23</sup>Na multiple-quantum magic-angle-spinning NMR could be readily correlated with sodium ion coordination environments. Furthermore, two complexes that had not been previously characterized structurally, disodium uridine-3'-monophosphate and a disodium uridine-3'-monophosphate/disodium uridine-2'-monophosphate mix, were identified by solid-state NMR. A spectroscopic assignment of the four sites of an additional salt, disodium adenosine-5'-triphosphate trihydrate, is also presented and discussed within the context of creating a general approach for the spectroscopic assignment of multiple sites in sodium nucleotide complexes. Copyright © 2006 John Wiley & Sons, Ltd.

**KEYWORDS:** NMR; MQMAS; <sup>23</sup>Na spectra; ATP; nucleotide binding motifs; REDOR; quadrupolar relaxation

## INTRODUCTION

Metal ions play important roles in both the structure and function of nucleotides and nucleic acids, which in typical biological environments behave as anionic polyelectrolytes.<sup>1,2</sup> Additionally, the implication of metal ions in the function of catalytic RNA has generated much interest in the study of metal–nucleic acid interactions.<sup>1–4</sup> Few spectroscopic techniques have been developed to investigate many of the metals that are important for nucleic acid structure and function, with sodium and magnesium serving as prominent examples. As a result, there is considerable interest in developing methodologies that will enable the study of ions such as sodium, which are EPR and optically silent. Most of the structural information available for these ions in biologically relevant environments comes from X-ray

crystallography, which has enabled many different sodium coordination environments to be identified. More recently it was shown that solid-state NMR studies could contribute significantly to the understanding of sodium DNA interactions, as well as of sodium ions interacting with nucleotides in solid crystalline samples of sodium nucleotide complexes.<sup>5–8</sup> This has been largely aided by ongoing developments of high-resolution solid-state NMR techniques that are capable of distinguishing among chemically inequivalent kinds of half-integer quadrupole nuclei – a class of nuclei to which the spin-3/2 <sup>23</sup>Na nucleus belongs – even when dealing with powdered samples.<sup>9,10</sup> In particular, the multiple-quantum magic-angle-spinning (MQMAS) technique, which allows for the determination of the nuclear quadrupole coupling parameters and the determination of isotropic chemical shifts under highly resolved conditions,<sup>11–14</sup> has been actively exploited in this context. In the present work, we further discuss the use of this and of related solid-state NMR techniques when attempting to spectroscopically probe sodium sites in solid samples of nucleotides cocrystallized with such ions. In particular, we discuss the possibility of combining multiple complementary spectroscopic approaches in order to classify and assign sites in these systems, utilizing the well-studied case of the sodium salt of ATP as a model.

<sup>†</sup>Dedicated to Professor David M. Grant of the University of Utah on the occasion of his 75th birthday, in recognition of the outstanding contributions he has made to the methodology of nuclear magnetic resonance and its application to a wide range of chemical topics over a long period of time.

\*Correspondence to: Lucio Frydman, Department of Chemical Physics, Weizmann Institute of Science, Rehovot, 76100, Israel.  
E-mail: lucio.frydman@weizmann.ac.il  
Contract/grant sponsor: Israel Science Foundation; Contract/grant number: 296/01.  
Contract/grant sponsor: National Institutes of Health; Contract/grant number: GM72565.  
Contract/grant sponsor: NIH Postdoctoral Fellowship; Contract/grant number: GM20417.

## EXPERIMENTAL

This study relied on the use of high-resolution solid-state NMR methodologies to study five sodium nucleotide

complexes: disodium deoxycytidine-5'-monophosphate heptahydrate (**1**); disodium deoxyuridine-5'-monophosphate pentahydrate (**2**); disodium uridine-3'-monophosphate (**3**); the system arising from an equimolar mixture of disodium uridine-3'-monophosphate/disodium uridine-2'-monophosphate (**4**) and disodium adenosine-5'-triphosphate trihydrate (**5**). Data for such complexes were acquired on home-built 7.1 T and 11.7 T NMR spectrometers, utilizing Tecmag pulse programmers and multiple-resonance homodyne radio frequency hardware. A three-channel Chemagnetics 4 mm MAS probe was used for all work at 7.1 T, while a Varian T3 double-resonance probe was used for all experiments at 11.7 T. MQMAS experiments were performed as previously described<sup>13,14</sup> utilizing either two-pulse or full-echo split-t1 sequences, modified in all cases so as to incorporate a fast amplitude modulation pulse shaping for the triple- to single-quantum conversion pulse stage.<sup>15,16</sup> All <sup>23</sup>Na shifts were externally referenced to aqueous NaCl, either by calibration with a NaCl (aq) standard or by monitoring solid NaCl and setting the resulting peak at 7.2 ppm.

Samples **1**, **2**, **3** and **4** were purchased from Sigma; each of them was dissolved in minimal amounts of water and recrystallized by vapor diffusion of acetone at 4 °C. Sample **5** was obtained as a 99% powdered solid from Sigma and was recrystallized from mixtures of H<sub>2</sub>O/dioxane and D<sub>2</sub>O/dioxane as described by Kennard *et al.*<sup>17</sup> **5** was also monitored using the sample as-purchased, without further purification or recrystallization. The 4-mm NMR rotors used in all experiments were loaded with approximately 35–40 mg of the nucleotide complex. All experiments at 11.7 T were performed while maintaining the sample temperature in the range of 10–15 °C in order to prevent, or in some cases slow down, sample degradation. Samples investigated at 7.1 T were studied at room temperature. When necessary, experimental lineshapes were fitted using custom-written simulation packages.

## RESULTS

### Overall <sup>23</sup>Na NMR features of the nucleotidic salts

Complex **1** contains two inequivalent sodium sites within the asymmetric unit, as determined by X-ray crystallographic analysis<sup>18</sup> and subsequently confirmed by solid-state NMR analyses.<sup>6,19</sup> One of the sodium ions (Na1) is coordinated by six water ligands in a nearly octahedral geometry, while the second sodium ion (Na2) is coordinated by five water ligands, four of which are shared with Na1 forming a dimeric structure (Fig. 1). <sup>23</sup>Na MAS (Fig. 2) and MQMAS (Fig. 3) NMR spectra clearly reveal a pair of spectral peaks for complex **1**. Analysis of these spectra allows for the following estimate of the quadrupolar ( $e^2qQ/h$ ,  $\eta$ ) and isotropic chemical shift ( $\delta_{\text{iso}}$ ) parameters. (As a matter of convention, we choose to number peaks throughout this study as they appear in the <sup>23</sup>Na isotropic shift domain of their 7.1 T MQMAS spectra and in order of decreasing frequency, i.e. left to right as data are displayed in Figs 2 and 3.) For peak 1:  $e^2qQ/h = 0.85$  MHz,  $\eta = 0.7$ ,  $\delta_{\text{iso}} = 0.1$  ppm; for peak 2:  $e^2qQ/h = 2.3$  MHz,  $\eta = 0.9$ ,  $\delta_{\text{iso}} = -3.7$  ppm. Peak 1 is then assigned to Na1 and peak 2

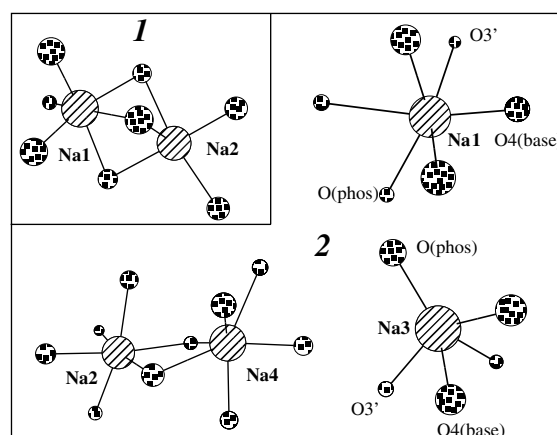


**Figure 1.** Coordination environments of the sodium sites in salts **1** and **2**, as derived from the crystal structures reported in Refs 18, 20, 21. Only the ions (⊗) and their inner-sphere oxygen donors (⊕) are shown; unlabeled oxygen atoms derive from coordinated waters of hydration.

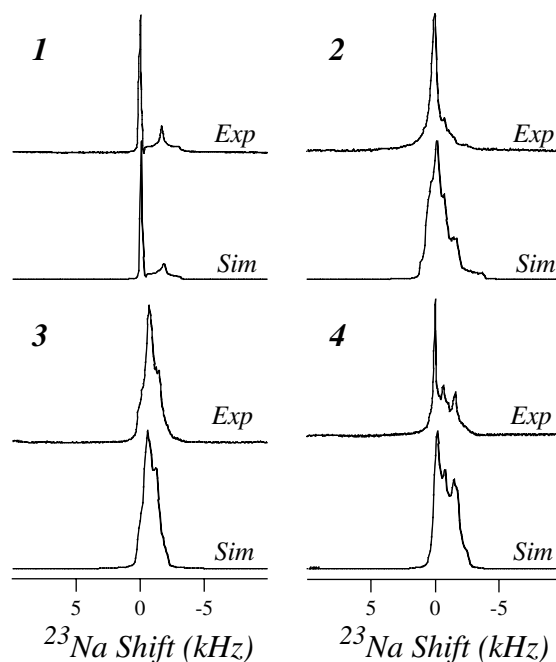


**Figure 2.** <sup>23</sup>Na MAS NMR spectra collected for complexes **1–4** at 11.7 T and at a spinning rate of 10 kHz. A single 0.7  $\mu$ s pulse was used in order to minimize potential lineshape distortions arising from quadrupolar nutation effects. The simulations shown underneath each spectrum are the result of extracting the individual quadrupolar and isotropic shift site parameters from the corresponding MQMAS data (Fig. 3) and then coadding the individual MAS powder lineshapes under the assumption of equipopulated sites. Differences can be noticed for complexes **2** and **4** between the intensities expected from the MQMAS parameters and those that are experimentally observed. We believe that this reflects a partial dynamical averaging that affects more strongly those sites with small  $e^2qQ/h$  values – coordinated as they are to more and more mobile water molecules – which enhances their relative contribution to the single-pulse MAS spectra.

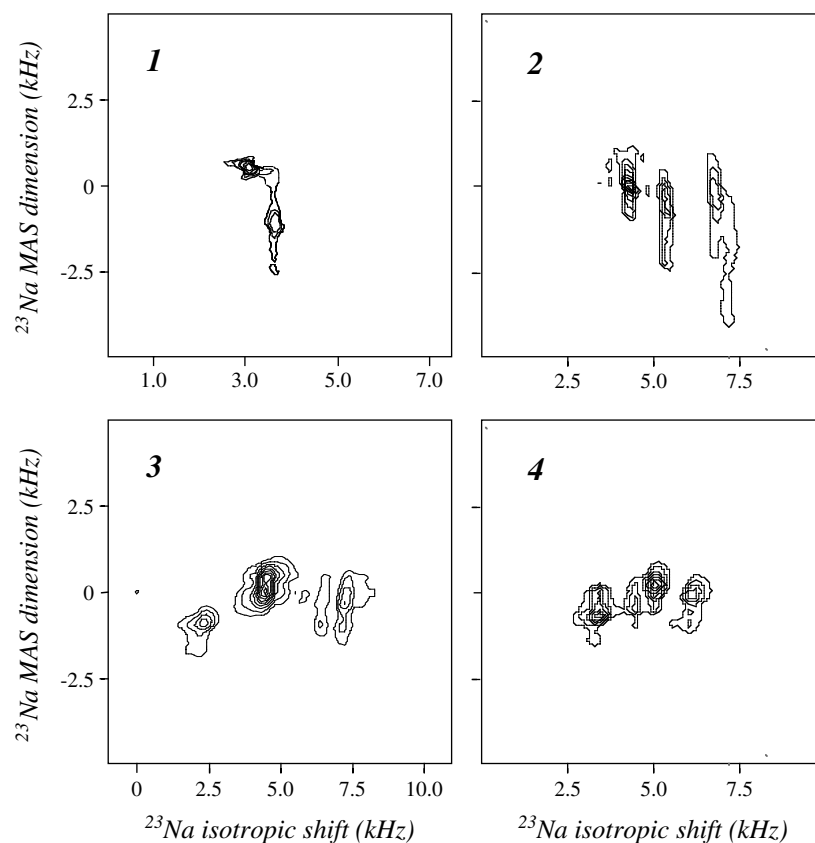


**Figure 3.** MQMAS NMR spectra collected on complexes 1–4. As for Fig. 2, these data were recorded on a home-built 11.7 T NMR spectrometer operating at a 132.3 MHz  $^{23}\text{Na}$  resonance frequency, utilizing a varian T3 double-resonance probe, two-pulse phase-modulation (TPPM)  $^1\text{H}$  decoupling throughout the sodium evolution periods,<sup>22</sup> and a 10.0 kHz sample spinning frequency. In all cases, sample temperatures were maintained at 15 °C by preregulating the gas stream used for the sample spinning.

is assigned to Na2, with the assignment based on the small nuclear quadrupole coupling constant expected for the highly symmetric octahedral site (Na1) and the much larger nuclear quadrupole coupling constant expected for the pentacoordinate site (Na2). These results are consistent with previous solid-state NMR analyses.<sup>6</sup>

Complex 2 contains four crystallographically inequivalent sodium sites within the asymmetric unit,<sup>20,21</sup> whose environments are depicted in Fig. 1. Two of the four sites are coordinated by shared water molecules in distorted octahedral environments (Na2 and Na4) with Na4 in what might be best described as a distorted trapezoidal bipyramidal geometry. The remaining two sodium sites derive several ligands from the nucleotide. Na1 donors include a phosphate oxygen ligand, the 3' oxygen of the ribose ring and the carbonyl oxygen (O4) of the uridine base, plus three additional water ligands – all this leading to a distorted octahedral geometry. Na3 is the only pentacoordinate site; it binds to a phosphate oxygen ligand, to the 3' oxygen of the ribose ring, to the carbonyl oxygen O4 of the uridine base and to two coordinated waters. The 1D  $^{23}\text{Na}$  MAS NMR spectrum of this salt at 7.1 T is hopelessly complex (Fig. 2, 2); the MQMAS NMR spectrum by contrast clearly reveals four peaks (Fig. 3) with the following spectral parameters: peak 1:  $e^2qQ/h = 1.9$  MHz,  $\eta = 0.8$ ,  $\delta_{\text{iso}} = -0.1$  ppm; peak 2:  $e^2qQ/h = 2.4$  MHz,  $\eta = 0.7$ ,  $\delta_{\text{iso}} = 0.0$  ppm; peak 3:  $e^2qQ/h = 2.3$  MHz,  $\eta = 0.6$ ,  $\delta_{\text{iso}} = 3.4$  ppm; peak 4:  $e^2qQ/h = 3.0$  MHz,  $\eta = 0.9$ ,  $\delta_{\text{iso}} = -0.1$  ppm.

Peak 1 can be assigned to Na2, which is the most highly symmetric among all sodium coordination environments, while peak 4 is assigned to Na4 as this is an ion in a very distorted trapezoidal bipyramid. An assignment of the remaining sodium sites could be made on the basis of symmetry arguments alone, but this is not necessarily a reliable approach. Further insight into the relations between the observed quadrupole couplings of this complex and sodium environments can be found in the recent work of Wong and Wu.<sup>6</sup>

A previous crystallographic analysis of complex 3 in its tetrahydrate form revealed two crystallographically inequivalent sodium ions within the asymmetric unit.<sup>21</sup> This X-ray study concluded that uridine-3'-monophosphate could only form analyzable single crystals when the complex was crystallized from a mixture of the 3'-monophosphate and the 2'-monophosphate isomers. Yet, solid-state MAS and MQMAS NMR spectra collected following a suitable crystallization of solely the 3'-UMP isomer clearly reveal four highly defined peaks (Fig. 3, 3). Joint analysis of these spectra suggests four sodium sites in the powder with the following parameters: peak 1:  $e^2qQ/h = 2.0$  MHz,  $\eta = 0.8$ ,  $\delta_{\text{iso}} = -4.7$  ppm; peak 2:  $e^2qQ/h = 1.3$  MHz,  $\eta = 0.7$ ,  $\delta_{\text{iso}} = 2.0$  ppm; peak 3:  $e^2qQ/h = 2.5$  MHz,  $\eta = 0.5$ ,  $\delta_{\text{iso}} = 2.0$  ppm; peak 4:  $e^2qQ/h = 2.2$  MHz,  $\eta = 0.85$ ,  $\delta_{\text{iso}} = 4.1$  ppm. This presence of multiple well-defined sites suggests the presence of either a crystalline structure different from

that determined in the previous X-ray study or of two or more polymorphic forms. By comparing the spectral parameters of **3** with those determined for **1** and **2**, it appears likely that peaks 3 and 4 in 3'-UMP – with their large quadrupole couplings – derive from either hexacoordinated sites directly linked to the nucleotide or alternatively from pentacoordinated environments. Peak 2, on the other hand, has quadrupole parameters that are similar to those that have been assigned to Na(H<sub>2</sub>O)<sub>6</sub> in an octahedral coordination environment for complexes **1** and **2**. Interestingly, when investigating the crystalline solid obtained by performing an identical crystallization procedure as that used for **3** but with a mixture of uridine's 3'-monophosphate and 2'-monophosphate isomers (complex **4**), four peaks are revealed – none of which appear to be in common with those of **3**. The spectral parameters for this form were estimated from the spectra shown in Figs 2 and 3 and are as follows: peak 1:  $e^2qQ/h = 1.9$  MHz,  $\eta = 0.8$ ,  $\delta_{\text{iso}} = -2.4$  ppm; peak 2:  $e^2qQ/h = 2.1$  MHz,  $\eta = 0.5$ ,  $\delta_{\text{iso}} = -0.4$  ppm; peak 3:  $e^2qQ/h = 1.7$  MHz,  $\eta = 0.7$ ,  $\delta_{\text{iso}} = 2.0$  ppm; peak 4:  $e^2qQ/h = 2.0$  MHz,  $\eta = 0.8$ ,  $\delta_{\text{iso}} = 3.0$  ppm. The presence of four inequivalent sites (as opposed to the two reported by X rays for this mixture) indicates that an entirely new crystal lattice has been formed in the presence of the pair of isomers. It is worth noting that the peaks of **4** seem to be somewhat broader in the isotropic dimension than the peaks of either **1** or **2**. This could be the result of less-than-perfect environments, yet it is still a much more crystalline behavior than that observed for amorphous samples (*vide infra*). Both complexes **3** and **4** were observed to rapidly degrade during the NMR analysis, presumably as a result of the rigors of sample spinning. As a result of such degradation, MQMAS lineshapes broadened and became mostly featureless, displaying little evidence of individual sites. With the sample temperature maintained at 10 °C, approximately 8 h of data acquisition was possible before the samples showed these signs of degradation.

The results obtained for complexes **1–4** offer insight into the range of values expected for the nuclear quadrupole and chemical shift parameters of sodium ions interacting with nucleotides in a crystalline environment. In favorable cases, such as for complex **1** and **2**, partial or full assignments of the resolved resonances can be made on the basis of symmetry and structural arguments alone – particularly with the benefit of the growing amount of biological sodium NMR data currently available in the literature.<sup>23</sup> However, as the multiple sites in complexes **1–4** illustrate, measuring <sup>23</sup>Na NMR parameters alone may only allow for a description of the sodium coordination environments in a minority of cases, particularly given the small range of <sup>23</sup>Na NMR's chemical shift and the variability of its quadrupole couplings. As a result, we decided to explore the possibility of aiding in the assignment of sites via the use of ancillary spectroscopy-based approaches. This exploration was focused on **5** (Fig. 4) because of the abundant structural information available for this disodium 5'-ATP complex and because of its diversity in coordination geometries and inner-sphere donors.

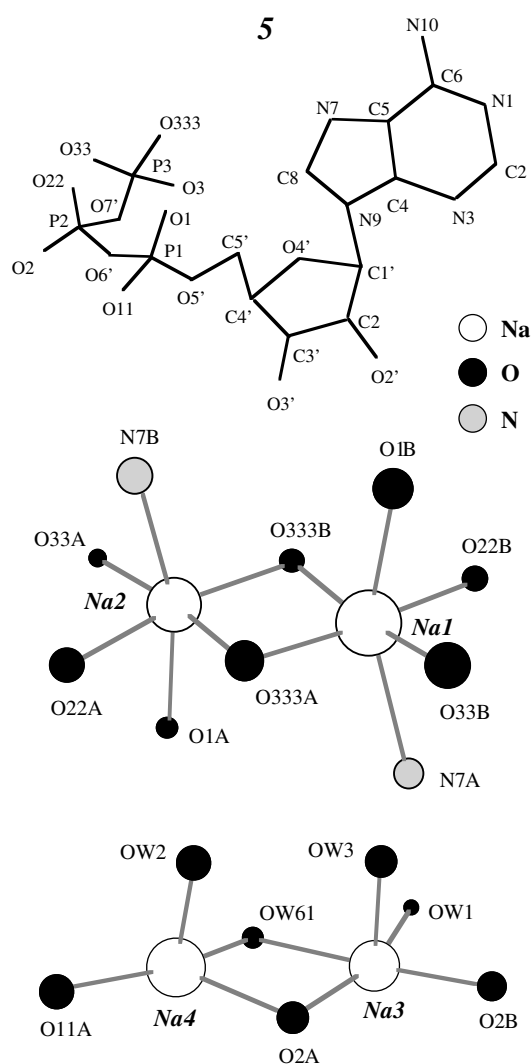


**Figure 4.** Illustration of the various sodium binding motifs exhibited by complex **5**, as presented by the crystal structure of Sugawara *et al.*<sup>24</sup> OW62 (not shown), highly disordered and distributed over two positions, completes the coordination environment of Na4.

### Solid-state NMR of disodium adenosine-5'-triphosphate trihydrate

The sodium nucleotide complex **5** was first investigated crystallographically by Kennard *et al.*,<sup>17</sup> who found four sodium ions, two ATP molecules and six waters coexisting within the asymmetric crystalline unit in the trihydrate form of this complex. A subsequent study reported crystal structures for both dihydrate and trihydrate forms of Na<sub>2</sub>ATP.<sup>24</sup> This work of Sugawara *et al.* demonstrated that the crystal cell dimension *a* changes approximately linearly with the level of relative humidity and that a single crystal in a controlled environment will eventually transform from a trihydrate to a dihydrate at approximately 5% relative humidity. This interconversion between the two forms was also shown to be reversible for the single-crystal sample studied. This study also concluded that the previously reported assignments of Na4 and OW4 were interchanged in the original structure of Na<sub>2</sub>ATP trihydrate presented by Kennard *et al.*, highlighting the complications

experienced by crystallography to differentiate among these two isoelectronic structures. Another interesting feature revealed by these studies of the  $\text{Na}_2\text{ATP}$  complex was the existence of a dimeric sodium structure (Na1 and Na2) that is bridged by a pair of phosphate oxygens, with the remaining ligands derived from phosphate oxygens and base nitrogens of the pair of ATP molecules in the repeating dimeric unit (Fig. 4). The two remaining sodium ions of the repeating unit (Na3 and Na4) are also dimerized, thus playing a role in linking adjacent ATP units. After careful consideration, we chose to interpret the NMR data presented here in the context of the Sugawara *et al.* structure, rather than on the structure of Kennard *et al.* This is in contrast to what has been done in previous solid-state NMR analyses of this complex,<sup>6,25</sup> interestingly, the results presented in these previous analyses also differ significantly from our own solid-state NMR investigations on the complex.

The  $^{31}\text{P}$  MAS NMR spectrum of a recrystallized sample 5 (Fig. 5(a)) gives rise to the familiar triphosphate nucleotide spectrum, with three peaks arising from the chemically inequivalent alpha, beta and gamma phosphorus atoms.<sup>26</sup> In this particular case, five peaks are resolved because of the beta and gamma resonances being split into pairs of peaks with similar intensities, reflecting the differences in magnetic environments characterizing the beta and gamma phosphorus atoms within the two crystallographically inequivalent ATP molecules in the asymmetric unit. This is very much in contrast to the spectrum obtained for the sample as-purchased, in which at least six resonances are identified as a result of several polymorphs, hydration states and/or partially amorphous environments coexisting in the powder (Fig. 5(b)). When investigated by  $^{23}\text{Na}$  MAS NMR at

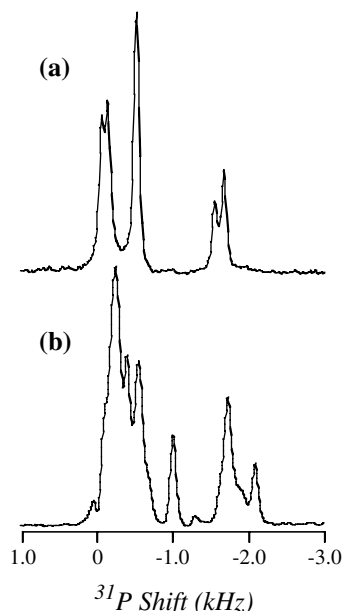


**Figure 5.** Centerband  $^{31}\text{P}$  cross-polarization magic-angle-spinning (CPMAS) NMR spectra of (a)  $\text{Na}_2\text{ATP}$  recrystallized from a water/dioxane solution and (b) as-purchased  $\text{Na}_2\text{ATP}$  without further recrystallization. Both spectra were obtained at 122.1 MHz (7.1 T) while spinning the sample at 7 kHz.

7.1 T, complex 5 gives rise to a single asymmetric peak for both the recrystallized as well as for the as-purchased sample (Fig. 6(a)–(c)). Samples recrystallized from dioxane solutions containing either  $\text{H}_2\text{O}$  or  $\text{D}_2\text{O}$  also give rise to only a small change in the lineshape, with slightly more resolution in the shoulder region observed for the  $\text{D}_2\text{O}$  sample (Fig. 6(b)).  $\text{H}_2\text{O}$ /dioxane- and  $\text{D}_2\text{O}$ /dioxane-crystallized samples also give similar  $^{23}\text{Na}$  MQMAS NMR patterns, but these are dramatically different from the 2D spectrum arising from the as-purchased powder (Fig. 7). Indeed, data obtained for both recrystallized samples clearly illustrate four well-defined sites in agreement with the crystallographic expectations. By contrast the as-purchased sample gives what appears to be two main isotropic peaks, flanked by additional minor resonances in close proximity to one another. It is quite likely that differences in hydration environments could be responsible for the different results reported in Fig. 7(a) and (b) *vis-à-vis* previous solid-state MQMAS NMR studies of  $\text{Na}_2\text{ATP}$ .<sup>6,25</sup> As mentioned, the crystallographic work of Sugawara *et al.* revealed a humidity-controlled reversible transition between the dihydrate and the trihydrate forms of  $\text{Na}_2\text{ATP}$ . Samples of 5 prepared as trihydrates were indeed observed to slowly degenerate after several days of data acquisition, with the degraded sample giving rise to changing features and to MQMAS NMR spectra that progressively resembled those of the as-purchased powder. As a result of this, fresh samples were used for all of the reported experiments; in all cases, the condition of the analyzed sample was initially assessed by  $^{31}\text{P}$  MAS NMR, which was found as a simple (though not an unquestionable) reporter of crystallinity.

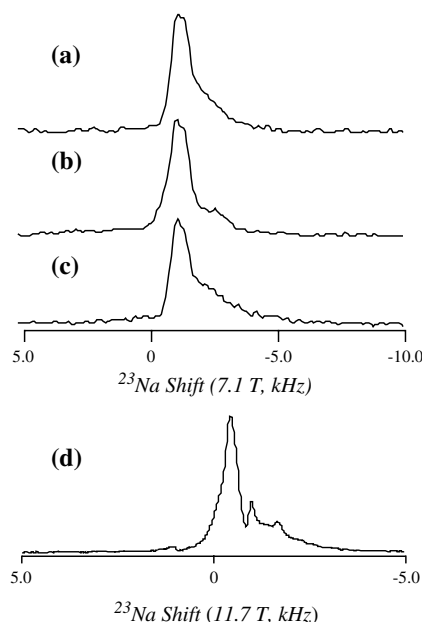


**Figure 6.** (a–c)  $^{23}\text{Na}$  MAS NMR spectra of  $\text{Na}_2\text{ATP}$  recorded at 79.78 MHz (7.1 T) with a sample spinning frequency of 8.0 kHz: (a) complex recrystallized from  $\text{H}_2\text{O}$ /dioxane; (b) complex recrystallized from  $\text{D}_2\text{O}$ /dioxane; (c) salt as-purchased and without further treatment. The spectrum illustrated in (d) was obtained from a  $\text{H}_2\text{O}$ /dioxane-crystallized sample at 132.36 MHz (11.75 T) with a sample spinning frequency of 12.0 kHz.

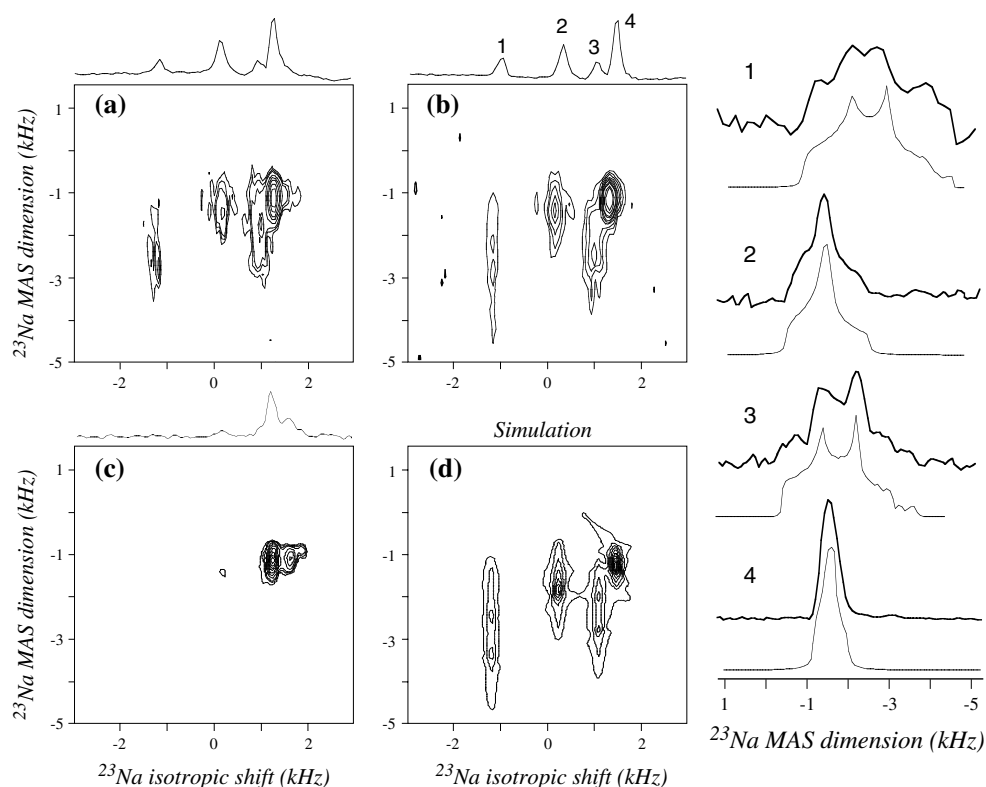


**Figure 7.** (a–c) Experimental  $^{23}\text{Na}$  MQMAS NMR spectra recorded from  $\text{Na}_2\text{ATP}$  at 79.78 MHz (7.1 T) with a sample spinning frequency of 10.0 kHz. (a) Sample recrystallized from  $\text{H}_2\text{O}/\text{dioxane}$ ; (b) sample recrystallized from  $\text{D}_2\text{O}/\text{dioxane}$ ; (c) as-purchased sample. The right-hand column compares simulated MAS lineshapes against the corresponding slices extracted for the four peaks resolved in the experimental spectrum (b), numbered 1–4 as they appear in the isotropic dimension. The 2D spectrum in (d) is a simulation arising from these best-fit parameters.

The experimental MAS and MQMAS results of **5** were analyzed as for all the previous complexes; shown on the right-hand panel of Fig. 7 (and in Fig. 7(d)) are numerical simulation of the MQMAS data collected from the  $\text{D}_2\text{O}$ -recrystallized sample (which offered slightly better resolution than its  $\text{H}_2\text{O}$ -crystallized counterpart). The four identified sites exhibited the following parameters (for peaks as they appear in order of ascending frequency in the isotropic domain of the 7.1 T MQMAS NMR spectrum: at a magnetic field of 11.7 T, the relative positions of peaks 3 and 4 reverse as a result of their relative quadrupole and chemical shift parameters (Fig. 9); however, we keep referring to the peaks using a numbering system consistent with their ordering at 7.1 T). Peak 1:  $e^2qQ/h = 2.3$  MHz,  $\eta = 0.5$ ,  $\delta_{\text{iso}} = -1.9$  ppm; peak 2:  $e^2qQ/h = 1.6$  MHz,  $\eta = 0.9$ ,  $\delta_{\text{iso}} = 1.6$  ppm; peak 3:  $e^2qQ/h = 2.1$  MHz,  $\eta = 0.5$ ,  $\delta_{\text{iso}} = 0.5$  ppm; peak 4:  $e^2qQ/h = 1.1$  MHz,  $\eta = 0.7$ ,  $\delta_{\text{iso}} = 0.0$  ppm.

Although the four peaks in the MQMAS spectrum of **5** are consistent with the existence of four inequivalent sodium sites within the crystal lattice, assigning these peaks to sodium sites identified by crystallography becomes a complex issue that cannot be unambiguously resolved on the basis of symmetry alone. Though the data of complexes **1** and **2** would indicate that peaks 1 or 3 could possibly be attributed to a five-coordinate site or to a distorted six-coordinate geometry, few other conclusions can be made by analogies with other compounds. As a result, we decided

to explore alternative ways in order to spectroscopically assign the four resolved peaks. One obvious feature to take advantage of is the disparate number of  $^{31}\text{P}$  dipolar contacts that each of the four sodium spins experiences. Both Na1 and Na2 derive five of their six ligands from phosphate oxygens in the triphosphate chains of the nucleotides within the asymmetric unit. As a result, both Na1 and Na2 have five phosphorus atoms within 4.0 Å and two additional contacts within 6.0 Å. Na3 and Na4 on the other hand have far fewer close contacts, with Na3 having two phosphorus atoms within 4.0 Å and Na4 having only one phosphorus within 4.0 Å. As a result, we expect a more significant dephasing of the Na1 and Na2 signals upon reintroducing the phosphorus dipolar couplings that have been averaged away by the MAS, while Na3 and Na4 are expected to experience significantly less dipolar dephasing. Because of the complexity of the spin system under consideration, these differences are not going to be discernible from a 1D  $^{23}\text{Na}$  MAS NMR trace such as that usually collected in spin-1/2 REDOR-type experiments;<sup>27</sup> neither can actual sodium–phosphorus distance information be expected to arise with a very high accuracy. And yet, a combination of MQMAS with the  $^{31}\text{P}$ – $^{23}\text{Na}$  rotational-echo double-resonance (REDOR) methodology could be employed as a spectral editing tool, with the expectation that the two classes of sodium sites mentioned above will be distinguished according to their differential dipolar couplings. MQMAS/REDOR-type experiments have in fact been used to investigate

dipolar interactions in this manner and have been shown to enjoy the resolution of the MQMAS experiment on one hand with the REDOR recoupling information on the other.<sup>28</sup>

Therefore, as an aid to the assignment of **5**, a <sup>23</sup>Na shifted-echo MQMAS experiment<sup>14</sup> was combined with a train of <sup>31</sup>P REDOR-dephasing  $\pi$ -pulses during an intermediate evolution time  $nT_r$  so as to reintroduce the <sup>23</sup>Na–<sup>31</sup>P coupling information (Fig. 8(a)). Figure 8(b) illustrates isotropic projections of such MQMAS-REDOR spectra with (S) and without ( $S_0$ ) the <sup>31</sup>P recoupling pulses; the subtraction of these two spectra ( $S_0 - S$ ) for  $n = 16$  is also shown. This difference spectrum reveals that dipolar dephasing has substantially diminished peaks 3 and 4, while having only a small effect on peaks 1 and 2. By measuring the volumes of the peaks in the 3D-type MQMAS/REDOR data sets (data not shown), it can be concluded that peaks 1 and 2 each achieve ( $S_0 - S$ )/ $S_0$  REDOR-dephasing values of  $0.10 \pm 0.05$ , while peaks 3 and 4 each achieve dephasings values of  $0.25 \pm 0.05$ . (The reported errors were estimated by integrating the noise of a representative volume of baseline and the data region whose decay was reliably reproducible.) As a result of this measurement, peaks 1 and 2 can be assigned to Na3 and Na4, while peaks 3 and 4 are assigned to Na1 and Na2. In both cases, individual sodium ions within each of these peak pairs remain indistinguishable by this methodology.

In addition to this MQMAS/REDOR site classification, variable temperature NMR was employed as a dynamical aid in assigning the peaks of the four sodium sites. Figure 9 displays two MQMAS data sets, obtained at +20 and –45 °C respectively. A distinct shift is found for peak 2, corresponding approximately to a 0.2 MHz increase in the nuclear quadrupole coupling constant. This result can be interpreted within the context of the disorder determined crystallographically in the work of Sugawara *et al.*<sup>24</sup> for the trihydrate form of Na<sub>2</sub>ATP, temperature factors of Na4, OW5, OW61 and OW62 were found to be near 20 Å<sup>3</sup> in agreement with the result of Kennard *et al.*<sup>17</sup> This extensive disorder in the crystallographic data is likely the result of local dynamics, and such dynamical processes can be expected to have a significant effect on the NMR spectrum. In the displayed variable temperature MQMAS data, only peak 2 is significantly influenced by lowering the sample temperature from +20 to –45 °C. As a result, we assign peak 2 as the signal arising from Na4, the sodium site that shows appreciable disorder in the crystal structure. Indeed, it is this very disorder that likely led to the difficulty in unambiguously identifying the position of Na4 in the original X-ray structure.<sup>17</sup> This variable temperature NMR result is also consistent with the above reported MQMAS/REDOR data, in which peaks 1 and 2 were determined to arise from either Na3 or Na4.

In an effort to gain more insight into the magnetic properties of the four peaks resolved in the MQMAS spectrum of **5**, the longitudinal relaxation times associated with each of the four resolved <sup>23</sup>Na peaks in its spectrum were also investigated. This investigation was carried out as a saturation-recovery experiment, with an initial total signal saturation, a subsequent parametric recovery period and

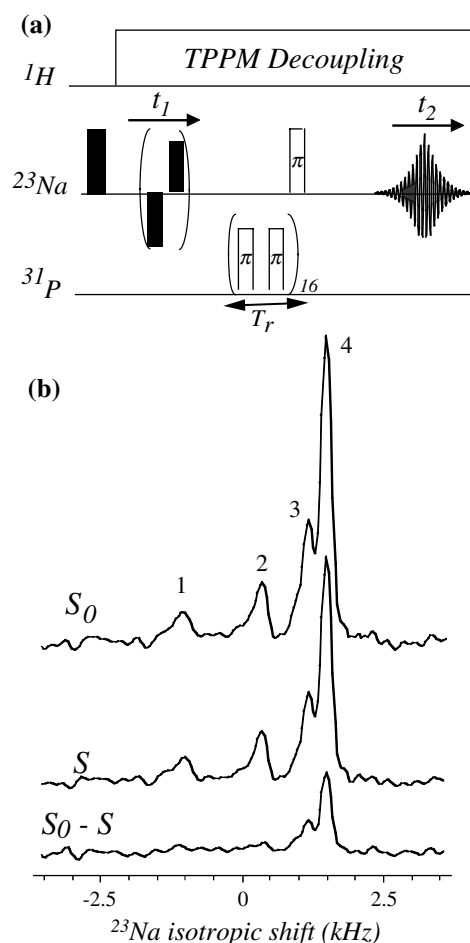


**Figure 8.** (a) REDOR-derived pulse sequence employed to assess sodium–phosphorus proximity via high-resolution <sup>23</sup>Na MQMAS NMR. In this case, the sample spinning frequency was set to 10.0 kHz and <sup>31</sup>P–<sup>23</sup>Na dipolar couplings were reintroduced by using pairs of <sup>31</sup>P  $\pi$  pulses centered at 1/4 and 3/4 of the rotor period  $T_r$  and applied over 16 rotor periods, amounting to a 1.6-ms long phosphorus recoupling time. (b) Isotropic projections retrieved in two <sup>23</sup>Na MQMAS data sets obtained with <sup>31</sup>P dephasing (S) and in an identical experiment without the <sup>31</sup>P pulses ( $S_0$ ). Subtracting S from  $S_0$  gives rise to the bottom trace. Peaks 1 and 2 are diminished in intensity by less than 10%, whereas peaks 3 and 4 are diminished by approximately 25%.

a final site-resolved acquisition accomplished by detecting the <sup>23</sup>Na signal within the framework of MQMAS. The resulting array of 2D MQMAS experiments, recorded as a function of the incremented recovery time, was processed by integrating each of the four peaks resolved in the 2D spectrum. Interestingly, it was then found that peaks 1 and 2 recovered approximately an order of magnitude faster than peaks 3 and 4 (Fig. 10). Fits to these data allowed for an estimation of the effective recovery time of the relaxation, which resulted to be very nearly a single exponential process with  $T_1$  values of 34, 31, 588 and 425 ms for peaks 1–4 respectively. These results are consistent with the other data presented in this work in that peak 1, assigned to Na3 and thereby to a site with many water protons nearby that undergo substantial dynamical processes, is expected to

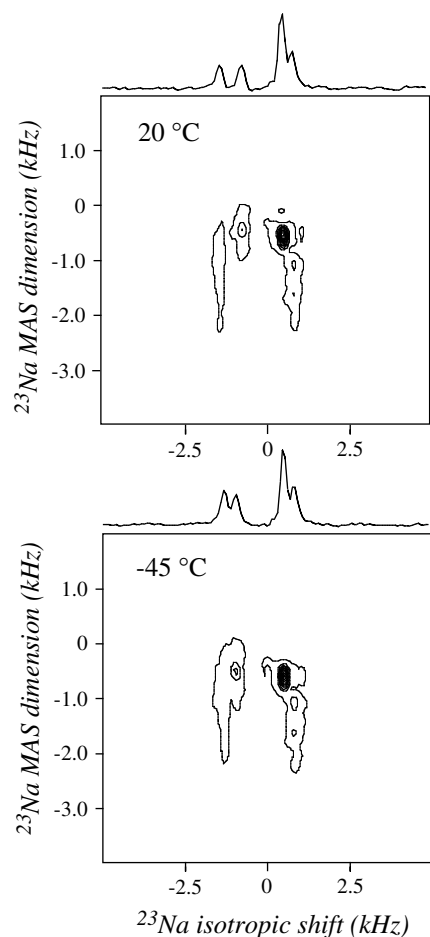


**Figure 9.** Comparison between  $^{23}\text{Na}$  MQMAS NMR spectra of  $\text{Na}_2\text{ATP}$  (11.7 T) acquired at 20 (top) and  $-45^\circ\text{C}$  (bottom) on a sample recrystallized from  $\text{H}_2\text{O}/\text{dioxane}$ . The spinning frequency was set to 10.0 kHz.

relax quickly. Peak 2, assigned to Na4 and the fastest relaxing signal in the set, is likewise influenced by the dynamical processes characterizing the bound waters. Peaks 3 and 4 relax with a rate approximately an order of magnitude slower than peaks 1 and 2, reflecting the much more rigid nature of the Na1/Na2 dimer.

## DISCUSSION

Complexes 1 and 2 illustrate how in favorable cases symmetry considerations alone can offer considerable insight into assigning the structures of the sodium sites that can be discerned by high-resolution  $^{23}\text{Na}$  solids NMR. In fact, in the very favorable case of complex 1,  $^{23}\text{Na}$  MAS NMR alone offered sufficient information – though in most cases the resolution enhancement offered by MQMAS or similar techniques will be the only way to obtain sufficient insight into the parameters of the individual sites. Complexes 3 and 4 further illustrate the utility of solid-state NMR analyses in identifying structures that may have otherwise been missed by single crystal crystallography.

The NMR data collected for complexes 3–5 also point out the limitations of symmetry-based quadrupolar assignments and the desirability to devise alternative spectroscopic

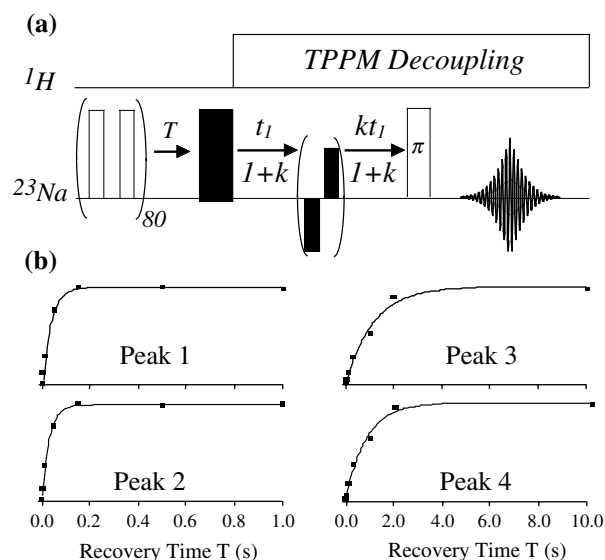


**Figure 10.** Saturation-recovery behavior observed by  $^{23}\text{Na}$  MQMAS for the different sites of  $\text{Na}_2\text{ATP}$ . (a) Pulse sequence assayed, which accomplishes the saturation by incorporating 80 pulses 3.0  $\mu\text{s}$  in duration separated by a delay of 336  $\mu\text{s}$ . These were followed by a recovery time  $T$  and a full-echo MQMAS acquisition. (b) Experimental results recorded at room temperature in a 7.1 T system upon setting the spinning frequency to 10.0 kHz. The squares denote the integrated volumes of the peaks as labeled in Fig. 7, and the smooth curves are single exponential fits of these data.

routes of classifying sites on the basis of structural and/or dynamical features. In the present work, we assumed that the availability of multiple crystallographic structures as well as the existence of dynamics made complex 5 particularly suitable for evaluating the potential utility of various hybrid MQMAS-based approaches. One such avenue to site classification took into consideration the disparate amounts of phosphorus dipolar couplings exhibited by the four observed sodium resonances. The resulting MQMAS/REDOR experiment allowed us to distinguish between the two classes of sodium sites, exhibiting differential dipolar interactions with  $^{31}\text{P}$  atoms in the phosphate chains. Further distinctions could be achieved by taking the temperature-dependence and relaxation behavior of the MQMAS-resolved isotropic NMR resonances into consideration. Independent evidence that peak 2 arose from Na4 could thus be obtained.

In spite of the potential shown by these hybrid approaches, none of the experiments applied on 5 allowed us to discriminate which of peaks 3 and 4 actually arose from sites Na1 and Na2. The crystallographic work of both Kennard *et al.* and Sugawara *et al.* actually show a very high degree of analogy among the bond lengths and angles of these two sites, and although crystallography does not necessarily address the details of the sodium electronic structure, it is still surprising to notice how different the nuclear quadrupole parameters are for these two sites. To a certain extent, this observation is also seen in the calculated electric field gradient tensor components reported by Wong and Wu,<sup>6</sup> where  $e^2Qq_{zz}$  values for Na1 and Na2 are reported as  $-2.090$  and  $-1.437$  MHz respectively. The observation

of such disparate quadrupole couplings for Na1 and Na2 initially caused us to consider the possibility that the four observed peaks arise from five sites – a likely possibility if the dihydrate and trihydrate forms of the complex were coexisting, and if Na1 and Na2 had similar magnetic properties and gave rise to one peak. However, all of our studies lead us to believe that this is not the case. For example, simulations of the MAS and MQMAS patterns are satisfactory only if four sites with a 1:1:1:1 ratio are assumed. Furthermore, we were only able to observe one set of results throughout the lifetime of the sample, and as the complex experienced the rigors of MAS for several days, we observed only disorder rather than the distinct transition between tri- and dihydrate forms, which is observed crystallographically.<sup>24</sup> And so, because the signals observed arose from fresh samples prepared in the trihydrate form of Na<sub>2</sub>ATP, we were forced to conclude that we were unable to observe any distinct sample transition during the course of our analysis.

## CONCLUSIONS

Solid-state MQMAS NMR was confirmed as a viable probe for monitoring binding sites in crystalline sodium samples of biological environments. The nuclear quadrupole coupling constants show a general trend of increasing as a hexacoordinated complex becomes more distorted, as coordination numbers decrease from 6 to 5 or upon ligating the sodium directly to the nucleotide. This study also revealed crystalline environments that had not been previously characterized by other techniques. In general, all of the studied samples contained more than one sodium site. As a result, we decided to investigate avenues of site assignment on the thoroughly characterized Na<sub>2</sub>ATP complex in its trihydrate form. Partial assignment of the four sites of Na<sub>2</sub>ATP could be accomplished by incorporating REDOR, variable temperature and relaxation methodologies onto the basic MQMAS high-resolution experiment. And yet, it was found that further refinements are needed if a full suite of experiments capable of classifying the various sodium environments arising in biological solids is to be developed.

## Acknowledgements

This work was supported by the Israel Science Foundation (grant 296/01), the National Institutes of Health (GM72565) and the Ilse Katz Magnetic Resonance Center of the Weizmann Institute. C.V.G was supported by NIH Postdoctoral Fellowship GM20417.

## REFERENCES

1. Aoki K. In *Metal Ions in Biological Systems*, vol. 32, Sigel A, Sigel H (eds). Marcel Dekker: New York, 1996; 91.
2. Sigel H, Song B. In *Metal Ions in Biological Systems*, vol. 32, Sigel A, Sigel H (eds). Marcel Dekker: New York, 1996; 135.
3. Feig AL, Uhlenbeck OC. In *The RNA World*, (2nd edn), Gesteland RF, Cech TR, Atkins JF (eds). Cold Spring Harbor Laboratory Press: New York, 1999; 287.
4. McKay DB, Wedekind JE. *The RNA World*, (2nd edn), Gesteland RF, Cech TR, Atkins JF (eds). Cold Spring Harbor Laboratory Press: New York, 1999; 265.
5. Rovnyak D, Baldus M, Wu G, Hud NV, Feigon J, Griffin RG. *J. Am. Chem. Soc.* 2000; **122**: 11 423.
6. Wong A, Wu G. *J. Phys. Chem. A* 2003; **107**: 579.
7. Wong A, Fettinger JC, Forman SL, Davis JT, Wu G. *J. Am. Chem. Soc.* 2002; **124**: 742.
8. Wong A, Wu G. *J. Am. Chem. Soc.* 2003; **125**: 13 895.
9. Frydman L. *Annu. Rev. Phys. Chem.* 2001; **52**: 463.
10. Duer M. *Introduction to Solid State NMR Spectroscopy*. Blackwell Publishing: London, 2004.
11. Frydman L, Harwood JS. *J. Am. Chem. Soc.* 1995; **117**: 5367.
12. Medek A, Harwood JS, Frydman L. *J. Am. Chem. Soc.* 1995; **117**: 12 779.
13. Amoureux JP, Fernandez C, Frydman L. *Chem. Phys. Lett.* 1996; **259**: 347.
14. Massiot D, Touzo B, Trumeau D, Coutures JP, Virlet J, Florian P, Grandinetti PJ. *Solid State NMR* 1996; **6**: 73.
15. Madhu PK, Goldbourt A, Frydman L, Vega S. *Chem. Phys. Lett.* 1999; **307**: 41.
16. Madhu PK, Goldbourt A, Frydman L, Vega S. *J. Chem. Phys.* 2000; **320**: 448.
17. Kennard O, Isaacs NW, Motherwell WDS, Coppola JC, Wampler DL, Larson AC, Watson DG. *Proc. R. Soc. London, Ser. A* 1971; **325**: 401.
18. Pandit J, Seshadri TP, Viswamitra MA. *Acta Crystallogr.* 1983; **C39**: 342.
19. Grinshtein J, Grant CV, Frydman L. *J. Am. Chem. Soc.* 2002; **124**: 13 344.
20. Viswamitra MA, Seshadri TP, Post ML. *Nature* 1975; **258**: 542.
21. Viswamitra MA, Seshadri TP, Post ML. *Acta Crystallogr.* 1980; **B36**: 2019.
22. Bennett AE, Rienstra CM, Auger M, Lakshmi KV, Griffin RG. *J. Chem. Phys.* 1995; **103**: 6951.
23. Goldbourt A, Madhu PK. *Annu. Rep. NMR Spectrosc.* 2004; **54**: 81.
24. Sugawara Y, Kamiya N, Iwasaki H, Ito T, Satow Y. *J. Am. Chem. Soc.* 1991; **113**: 5440.
25. Ding S, McDowell CA. *Chem. Phys. Lett.* 2000; **320**: 316.
26. Un S, Klein MP. *J. Am. Chem. Soc.* 1989; **111**: 5119.
27. Gullion T, Schaefer J. *J. Magn. Reson.* 1989; **81**: 196.
28. Fernandez C, Lang DP, Amoureux JP, Pruski M. *J. Am. Chem. Soc.* 1998; **120**: 2672.